OPTIMIZATION OF CANARD CONFIGURATIONS — AN INTEGRATED APPROACH AND PRACTICAL DRAG ESTIMATION METHOD

I.M. Kroo and T. McGeer
Stanford University
Stanford, Calif. USA

Abstract

A fundamental analysis of subsonic canard configurations illustrates some of the problems associated with such designs and difficulties encountered in their optimization. A general solution for minimum induced drag as a function of span ratio, vertical gap, and relative surface lifts is presented. Stability and trim requirements, together with the system geometry then determine the total induced drag and practical conclusions follow when structural weight and stalling speed constraints are added. Required chord and twist distributions are determined, illustrating the problems associated with multiple design points. Unlike conventional configurations, the canards' geometric variables associated with optimal solutions to each of the above problems vary widely, showing great sensitivity to constraints and off-design operation.

I. Introduction

A recent resurgence of interest in canard configurations for subsonic aircraft is evidenced by the appearance of a variety of such designs in general aviation, business aircraft, and some proposed commuters and has led to a need for practical, preliminary design tools. The great variation in these designs contrasts sharply with the relative standardization of aft-tail configurations and suggests that some aspects of their design may be less well-understood. Much of the literature dealing with subsonic canard configurations has focussed on methods for predicting the aerodynamic characteristics of a particular geometry. A variety of papers[1-3] has addressed the question of minimum induced drag, with and without trim and root bending moment constraints, but with a number of additional constraints imposed to simplify the analysis. Although such studies are useful, conclusions regarding "optimal" configurations are valid in a very restricted sense. For canard / wing combinations, to a greater extent than for conventional designs, optimal solutions show great sensitivity to the choice of goal function and imposed constraints. Because of this sensitivity, optimal solutions to the more restricted problems (e.g. minimum induced drag with fixed span) differ significantly from those which result from an integrated approach including total drag, weight, and stalling speed considerations.

Beginning with a general analysis of the minimum induced drag of two non-coplanar lifting surfaces which yields a simple relation between total induced drag and the system geometry, the effects of various constraints are illustrated as stability and trim constraints are imposed, followed by structural weight and stalling speed requirements. The analysis applies equally well to canard and conventional configurations and demonstrates important differences in relative performance.

II. Minimum Induced Drag

The problem of computing the induced drag of two non-coplanar lifting surfaces is discussed in a number of previous papers utilizing three basic techniques: conformal mappings[4], vortex lattice methods[2], and variations of Prandtl's biplane equation[3,5-9]. Although vortex lattice and a variety of panelling methods provide accurate results for a given configuration, in the context of preliminary design optimization with large numbers of design variables, even mildly computation-intensive codes are wholly unsatisfactory. A large gap exists between these refined methods and the biplane equation of Prandtl[5] which is also widely used because of its simplicity:

$$D_i = \frac{{L_w}^2}{q\pi {b_w}^2} + \frac{2L_t L_w \sigma}{q\pi b_w b_t} + \frac{{L_t}^2}{q\pi {b_t}^2} \qquad (1)$$

The limited number of variables and algebraic form of equation (1) (where σ is a function of span and vertical gap ratios only) make it particularly useful. Many recent analyses of trimmed drag for conventional and canard designs and of optimum center of gravity position and tail load have been based on this equation and reflect the utility of such a simple approach.

The key assumption underlying equation (1) is that each surface is elliptically loaded. However, when operating in the downwash field of a highly-loaded canard, the wing's lift distribution tends to be shifted outboard because of the downwash directly behind, and upwash outboard, of the canard. The wing, of course could be twisted to produce an elliptic load distribution in spite of this non-uniform downwash field, but, despite some confusion in the literature, the idealized individually-elliptic load distribution is often far from ideal. This is easily demonstrated in the case when the two surfaces are coplanar. Prandtl pointed out that, in this case, Munk's stagger theorem[10] permitted superposition of the individual loadings so that the system could be treated as a single wing for the purposes of induced drag calculation. The minimum induced drag is achieved when the total loading is elliptical over the larger span; and the wing's lift distribution is decreased inboard and increased outboard of the canard. This loading is in the same sense that the lift distribution of an untwisted wing is shifted when operating in the canard's downwash field and the loading change probably accounts for the overestimation of canard drag by equation (1) when compared with experiments[11].

Because of the limitation of equation (1) to elliptically loaded wings, several attempts have been made to generalize the expression to include more realistic distributions. The induced drag of systems with certain non-elliptic distributions of lift on one or both surfaces is computed in references 7 and 12. Some recent work[9] has also examined the induced drag of systems with one elliptically-loaded surface and one optimally loaded surface.

Rather than specify the shape of the surface lift distributions a priori, however, one can calculate those which minimize the total induced drag. This may be done by expanding the lift distributions in Fourier series,

$$l_w = \frac{4L}{\pi b_w} \sum A_{nw} sinn\theta_w \qquad (2)$$

$$l_t = \frac{4L}{\pi b_t} \sum A_{nt} sinn\theta_t$$

and solving for the coefficients which produce minimum drag. (Appendix I details the procedure by which the optimum distributions are computed.) Figure 1 shows that for some configurations, the shape of the optimal wing lift distribution may, indeed, differ greatly from elliptical. If the load carried by the smaller span is small, or if the vertical separation or span ratio is large the distributions again approach the isolated elliptic result.

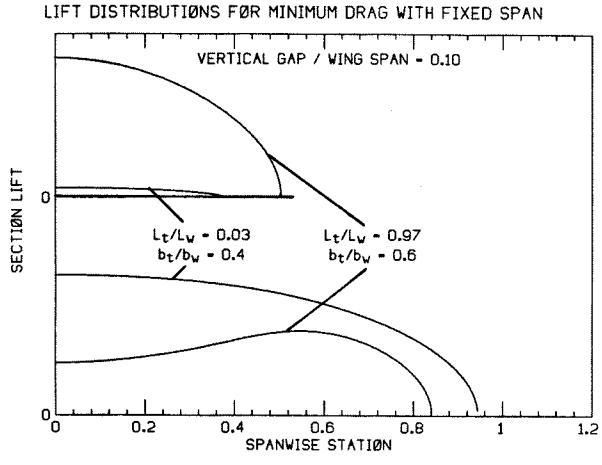

Fig. 1

The induced drag produced by this optimally loaded system may be written:

$$D_{imin} = \frac{{L_w}^2}{q\pi {b_w}^2}\sigma_w + \frac{2L_t L_w}{q\pi b_w b_t}\sigma_{wt} + \frac{{L_t}^2}{q\pi {b_t}^2}\sigma_t \qquad (3)$$

where the constants σ_w, σ_{wt}, and σ_t are functions only of span ratio, $\frac{b_t}{b_w}$, and dimensionless vertical gap, $\frac{h}{b_w}$.

The ratio of the minimum induced drag of this system to that of a single wing of the same span as the larger span, carrying the same total lift (span efficiency) is:

$$u = \frac{(1+\bar{L})^2}{\sigma_w + \frac{2\bar{L}}{\bar{b}}\sigma_{wt} + (\frac{\bar{L}}{\bar{b}})^2\sigma_t} \qquad (4)$$

with $\bar{L} = \frac{L_t}{L_w}$.

Unlike equation (1) in which the three terms consist of two self-induced drag terms and an interference term, all three terms of equation (3) contain both self-induced and interference effects. σ_{wt} and σ_t are plotted vs. span ratio, $\frac{b_t}{b_w}$ in figure 2. σ_w is not included as it is essentially 1.0 over a wide range of span and gap ratios (σ_w varies slightly in cases with large span ratios and small gaps but even in an extreme case with $\bar{h} = .05$ and $\bar{b} = 1.0$, $\sigma_w = .980$). It should also be noted that $\sigma_{wt} \simeq \sigma$, Prandtl's interference factor in equation (1), while σ_t differs greatly from 1.0 in the case of small span and gap ratios.

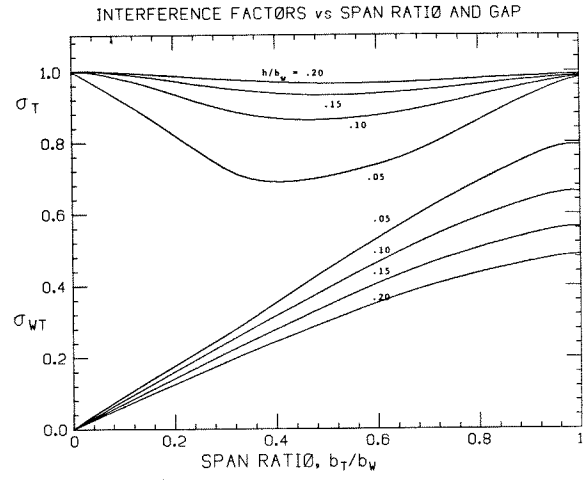

Fig. 2

So, equation (3) is similar to equation (1) differing primarily in the coefficient σ_t in the last term. This reflects the fact that the momentum imparted to a small mass of air by the canard may be redistributed by the wing over a larger mass of air. Thus, when $h = 0$ the wing is capable of redistributing the momentum over its entire span so that the minimum induced drag (regardless of canard load) is just that which would be produced by an single elliptically loaded wing carrying the same total lift. This explains the interesting result that for certain cases the interference terms are beneficial and the induced drag is actually lower than if the two wings were infinitely far apart. Equation (1), to the contrary, suggests that induced drag always decreases with larger vertical gap whenever $\bar{L}$ is positive.

Since $\sigma_t = 1$ when the wing is elliptically loaded, the minimum induced drag given by equation (3) may differ significantly from that given by equation (1). If, for example, $\bar{h} = .04$, $\bar{L} = .3$, and $\bar{b} = .4$, equation (3) gives $u = .885$, while if the surfaces were elliptically loaded $u = .802$. Differences become larger for smaller gaps and larger span loading ratios, $\frac{\bar{L}}{\bar{b}}$. Thus, although equation (3) may be used for estimating the induced drag of conventional, aft-tail configurations, it is especially useful for canard configurations which, because of stability and trim constraints, generally require larger values of $\frac{\bar{L}}{\bar{b}}$.

Figure 2 illustrates the rapid variation of σ_t for small vertical gaps. This decrease in σ_t reflects the substantial reduction in induced drag compared with the elliptically loaded case. Because of this sensitivity, however, the theoretical result that $u_{opt} = 1$ and is independent of $\bar{L}$ when no vertical gap is present, is not achievable in practical cases where h does not vanish completely.

In figure 3, the variation of induced drag factor, u , with span ratio is shown for various values of tail / wing lift ratio, $\bar{L} = \frac{L_t}{L_w}$. Even for this small value of vertical gap, ($\bar{h} = .05$) the value of u differs substantially from 1.0 when the smaller span is required to carry a significant portion of the total load. Although the induced drag of a system with no vertical gap and elliptic loading on each surface is symmetric in $\frac{L_t}{L_{tot}}$ (that is, the total drag is determined by the magnitude of tail lift and is the same for positively and negatively loaded tails), when the loading is chosen to minimize induced drag this is no longer the case and "down-loaded" tails incur a larger penalty.

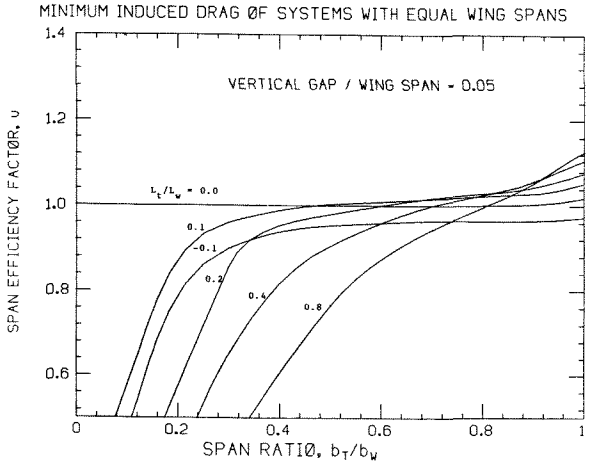

Fig.3

III. Minimum Trimmed Induced Drag

The requirements of stability and trim determine the lift ratio for a given configuration and have a strong impact on the induced drag of canard configurations. The condition for trim is:

$$L_f x_f - L_r x_r + q S_f c_f C_{macf} + q S_r c_r C_{macr} = 0$$

with x_f and x_r the distances from the center of gravity to to forward and rear surfaces' aerodynamic centers. For the purposes of this general discussion the effect of section camber and individual surface C_{mac} is omitted so that:

$$\frac{L_f}{L_r} = \frac{x_r}{x_f}$$

If the stability requirement is satisfied by requiring the center of gravity to lie ahead of the neutral point by a distance Δ (in units of the wing–tail separation, $x_f + x_r = 1$),

$$\frac{L_f}{L_r} = \frac{1 + \Delta - c1}{c1 - \Delta} \qquad (5)$$

with:

$$c1 = (1 + \frac{C_{L\alpha f}}{C_{L\alpha r}} \frac{S_f}{S_r})^{-1}$$

The ratio of lift curve slopes is influenced by interference effects; the canard reduces the wing's lift curve slope and the wing's trailing vortex system and bound vortex generally increase the canard's effectiveness. These interactions are most easily taken into account by applying Hayes' reverse flow theorem (cf. Ref.13). With this theorem it is possible to compute the effect of the canard's induced velocities on the wing's lift curve slope by evaluating the effect of the wing's downwash on the canard in reversed flow. The latter is much more easily accomplished, several approximate methods being readily available.

The ratio of lift curve slopes is thus determined by the surfaces' horizontal and vertical separation, spans, and areas. However, the ratio is principally determined by horizontal gap, span ratio, and area ratio. (In this paper we have assumed, for the purposes of computing lift curve slope ratio, that $AR_w = 10$ and horizontal gap $= 4$ wing chords.)

With these assumptions then, the lift ratio may be computed from equation (5) and substituted into equation (3) to obtain the minimum trimmed induced drag shown in figures 4 and 5.

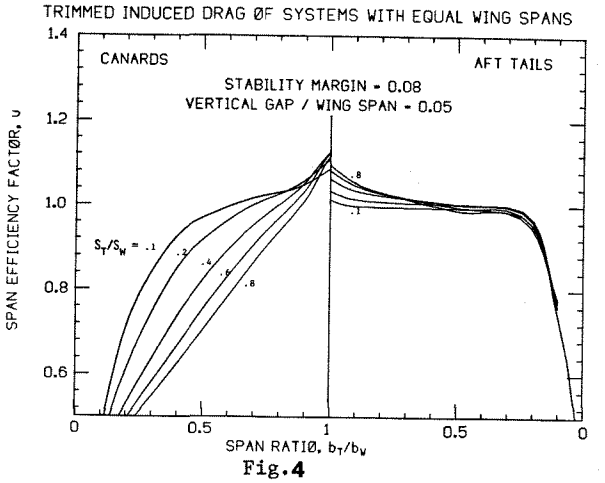

Fig.4

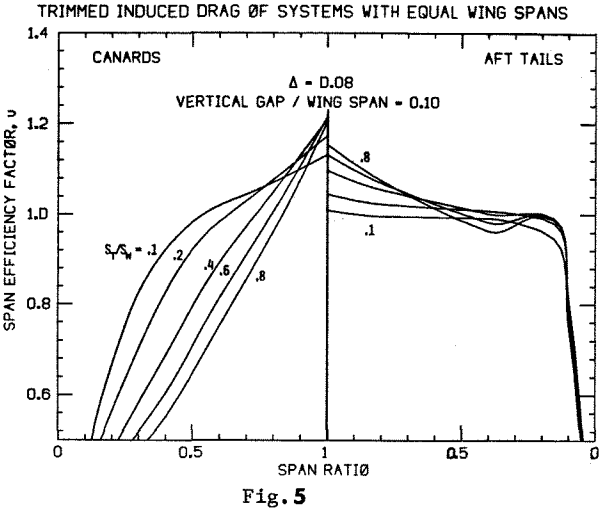

Fig.5

A stability margin, Δ, of .08 was chosen in this analysis. While this would correspond to a rather high stability level for the lifting system alone, destabilizing effects of the rest of the airframe make this static margin only moderate. The effect of section camber changes the results of this analysis in the same sense so that calculated tail loads are most representative of those which would be obtained at mid to aft center of gravity positions. Furthermore, although equation (3) applies to surfaces with or without sweep, the C_{mac} associated with a swept, twisted wing modifies the results of figures 4 and 5 slightly. The remaining discussion in this paper is, therefore, strictly applicable only to unswept surfaces.

From these figures it is apparent that although the Prandtl biplane equation overestimates the total induced drag, even the minimum induced drag solution leads to very low values of span efficiency, u, if the canard span is not large. By contrast, the minimum induced drag of aft-tail designs is rather insensitive to tail span over a wide range of tail sizes. So, although reducing the vertical gap reduces the induced drag in some cases, these are cases in which the span efficiency is very low. Thus, the induced drag of certain canard designs in figure 4 ($\bar{h} = .05$) is lower than the corresponding configuration with a larger vertical gap ($\bar{h} = .10$) in figure 5, but only for designs with $u < .8$. Similarly, the penalty in induced drag associated with "down-loaded" aft-tail configurations may be reduced by decreasing the vertical gap.

Among the conclusions apparent from these figures are:

1) To obtain values of u comparable to that of conventional designs, the canard span ratio must be large — .5 or greater.

2) In terms of induced drag with fixed span, canard span ratio should be large and, except for the highest span ratios, canard area ratio should be small.

3) Biplane / tandem designs lead to largest values of u for fixed span with $u = 1.2$ to 1.3 when large vertical gaps are available.

IV. Minimum Induced Drag with Fixed Weight

Despite their advantage in span efficiency, tandem configurations comprise a decidedly small minority of modern aircraft. That advantage, of course, is offset by structural weight – while a system with a small tail has higher induced drag than a tandem of the same *span*, for the same *weight* the wing span can be made sufficiently greater in the small-tailed system to overcome its lower u. To make a practical comparison between the induced drags of these, and any other lifting systems, one must fix not the span of the wing, but rather the weight of the system.

To proceed with this comparison, we need a method for calculating the relative structural weight of lifting systems. A multitude of factors have some bearing upon this calculation; however, only a few of these have a strong influence and a first analysis should isolate these primary factors for exclusive study. The major factors affecting the weight of a surface are its span, area, and total lift, its planform, and its lift distribution. (For the same total lift, a wing having relatively high tip loading, as is required for optimum span efficiency in a canard configuration, will be heavier than one having low tip loading.) All of these effects can be captured by modeling the lifting surface as a cantilever beam, in which the bending loads are carried by the spar caps.

If one applies this model to a wing having constant thickness-to-chord ratio and bending stress across the span, one finds that the weight per unit span can be written as:

$$w(y) = \frac{w_s \chi(y) S}{b} + \frac{w_b b M(y)}{\chi(y) S} \tag{6}$$

where $\frac{\chi(y)S}{b}$ is the local chord (which, for each surface in the lifting system, is normalized by the *total* area and the surface span). The terms account roughly for the weight associated with the skin and spar, respectively. To find the weight of a lifting system, one must integrate this formula across the two spans. The skin term simply integrates to $\mu_s S$. The spar term is most easily treated by decomposition into harmonics. Thus, the spar weight can be written as

$$W_b = \frac{w_b L {b_w}^3}{2S}\left(\sum_1^M A_{wm} \int_0^{\frac{\pi}{2}} \frac{M_{mw}}{\chi_w} sin\theta d\theta \right.$$

$$\left. + \bar{b}^3 \sum_1^N A_{tn} \int_0^{\frac{\pi}{2}} \frac{M_{mt}}{\chi_t} sin\theta d\theta \right) \tag{7}$$

where $\frac{b_w L}{2} M_{mw}(\theta)$, for example, is the moment due to the m^{th} harmonic of the wing lift.

It is convenient to non-dimensionalize this expression by introducing as a 'reference wing', a single surface having elliptical loading and planform, and carrying the same total lift. The weight relative to this surface may be written as

$$W = f_s S + \frac{f_b {b_w}^3}{S} \sum A_{wm} B_{wm} + \bar{b}^3 \sum A_{tn} B_{tn} \tag{8}$$

S,b_w, and W are now relative quantities. We have replaced w_b and w_s by f_b and f_s, which are the 'spar' and 'skin' weight fractions of the reference wing. (Note that $f_s = 1 - f_b$.) The B coefficients are the integrals in the formula for spar weight, scaled so that $B_1 = 1$ for an elliptical surface.

This weight formula obviously excludes many elements of a complete structural analysis, but it does satisfy our requirement for an index which realistically accounts for the most powerful effects. Let us now apply it to finding the minimum induced drag of a lifting system of fixed weight. Consider the choice of lift distributions. Although in some cases the lift distributions in the critical loading condition may differ from those for minimum induced drag, in systems having fixed twist distributions they will be approximately the same, since both conditions occur at high C_L. We will return to this point in section VI in regard to off-design performance.

Since minimum induced drag is achived with maximum $b^2 u$, not maximum u, the lift distributions calculated in the preceeding section do not produce minimum induced drag with fixed weight. By carrying more lift inboard than is

optimal for span efficiency, one can reduce the integrated bending moments, and so make the span larger for a given weight. Thus we must solve for minimum system drag with a weight constraint as a distinct problem. This problem is very much in the spirit of those treated by R.T. Jones[15,16] and Prandtl[14] on minimum drag of a wing with fixed bending moment. Here we will present a solution which extends these analyses in two respects: First, it involves a weight model which is sensitive to variations in section thickness (through variations in chord) as well as to the moment distribution. Second, it applies to a system of two interfering surfaces, rather than an isolated monoplane.

Appendix II gives the details of the analysis. It turns out that, with the weight and area of the system fixed, the solution is *independent* of the weight fractions f_b and f_s. Hence it depends only upon the tail span ratio, area ratio, lift ratio, and vertical gap, and (through the B coefficients) upon the planforms of the two surfaces. The first four of these parameters entered into the trimmed drag calculations of the preceeding section, but the planforms are new unknowns. Naturally, we want to choose the optimum planforms which for any surface, is that which maximizes span for a fixed weight (or, equivalently, minimizes weight for a fixed span). By differentiating with respect to chord in our formula for weight per unit span, one finds that chords proportional to the square root of the bending moment at each point satisfy the optimality condition. (Actually, if the surface area is fixed one has to modify the analysis, but the basic result is the same.)

Unfortunately, this planform always produces a section C_l distribution which increases monotonically toward the tip, since the bending moment always decreases from root to tip more quickly than does the lift. In fact the C_l becomes infinite at the tip, and very large over the outboard part of the surface – a situation which is obviously impractical. Spanwise pressure gradients, parasite drag, and ultimately stall preclude large variations in C_l across the span. One is forced to make C_l over the outboard part of a wing less than the average particularly to avoid tip stall. The natural way to accomodate this constraint is to place an upper bound on C_l which one can vary across the span. Not surprisingly, when one imposes such a constraint, the optimum chord becomes

$$c(y) = max\left(\frac{l(y)}{qC_{l_{bound}}}, k\sqrt{M(y)}\right)$$

with k scaled to give the correct surface area.

In the calculations here, we have imposed a C_l bound which varies linearly across the span, from 0.9 of the surface C_l at the tip to 1.2 at the root. Figure 6 shows the maximum b^2u which can be obtained, relative to the reference wing, within this constraint. The vertical gap is 0.05 and the stability margin 0.08; thus this figure is directly comparable to figure 3, which shows the results obtained with fixed span rather than fixed weight. The most obvious difference between the two is the shift in the optima from tandems to small tails and canards as anticipated. Also apparent is the increased sensitivity to the choice of tail area. Both canard and aft-tailed designs exhibit this sensitivity but for somewhat different reasons. In the case of aft tailed systems, the wing lift fraction is relatively insensitive to wing area. Consequently, decreasing the wing area simply reduces the size of the structure carrying the load, and to maintain a fixed weight the lift distribution must be shifted inboard or the span reduced – either way, b^2u suffers. When the area of the wing in a canard system is decreased, on the other hand, its lift drops more or less proportionately. However, the wing lift distribution required for optimum efficiency becomes increasingly tip-heavy, so again the choice is between reducing the wing span and making the efficiency sub-optimal. This conflict between the high wing tip loading required for maximum u, and the low tip loading required for maximum span, is an inherent disadvantage of canard configurations, and for this reason their drag relative to aft-tailed systems is higher with fixed weight than with fixed span.

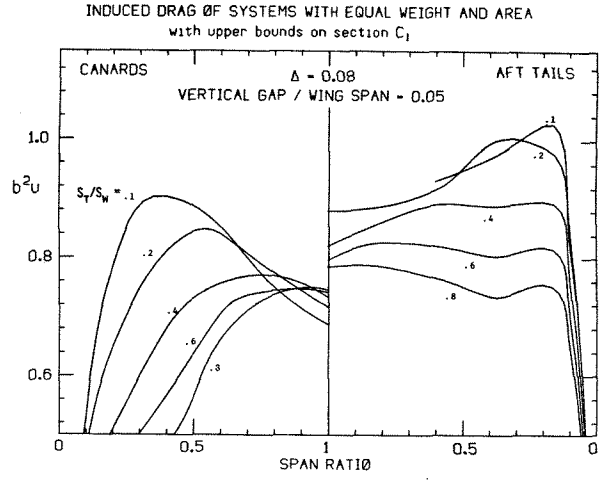

Fig. 6

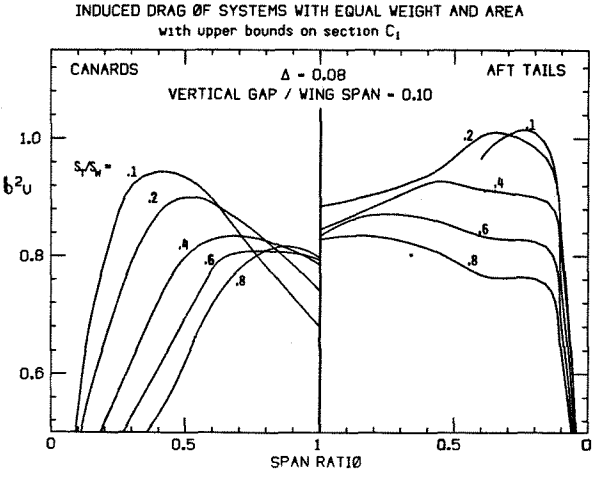

Fig. 7

As the vertical gap increases, the wing tip loading required for maximum u is reduced, and this conflict is alleviated. The relative position of canard systems therefore improves, as one can appreciate by comparing figure 6 and 7. The improvement is larger than the fixed span analysis would lead one to anticipate – in fact, for some systems u decreases with increasing gap. The fixed weight analysis, on the other hand, indicates that for minimum induced drag the gap of canard systems should be as large as possible.

It might be surprising that some of the systems plotted in figures 6 and 7 have values of b^2u greater than 1 – i.e. better than the reference monoplane. This does not mean that some two surface systems have inherently lower drag than a single wing, since we are comparing systems with optimum lift and planform to a wing with elliptical lift and planform. It does, however, indicate the advantages which the optimization offers. These will become more apparent if we compare systems designed for maximum b^2u with those designed for maximum u. Our sample aft–tailed system has a fairly high aspect ratio tail (span ratio 0.4 and area ratio 0.2). Our sample canard is larger, with span and area ratios of 0.6. The gap is 0.1 in both cases. Figure 5 showed the maximum u lift distributions for these configurations; figure 8 shows those for maximum b^2u. Note that the spans on each plot are scaled so that all of the systems would have the same weight. The most obviously different distributions are those over the wings in the canard systems. This difference is reflected in their relative span and span efficiency. The system designed for maximum b^2u has a span which is 25% greater than that of the maximum u system, while its u is lower by 15%. Its net advantage in induced drag is about 26%. The difference between the maximum b^2u and maximum u systems with aft tails is not quite so large but still substantial – the maximum b^2u configuration has a span greater by 9%, and u lower by 6%, so 11% lower drag overall. The sample canard system has 53% more drag than the aft-tailed version with maximum u lift distributions, and 30% higher drag when designed for maximum b^2u.

Figures 9 and 10 show the planforms of these systems Each surface has the same characteristic shape – over the outboard section, the chord is set by the C_l bound, and the contour follows the lift distribution. The area which is left over after the C_l constraint has been satisfied is concentrated at the root, where the chord varies with the square root of the bending moment. Although most manufacturing engineers would undoubtedly be unconvinced that these planforms — particularly of the wing in the canard configuration —are optimal, these 'ideal' shapes serve as useful approximations to those which might be practically employed. The drag reduction offered by maximum b^2u design, compared to the more familiar maximum u design is substantial, and advantages of the order indicated here are within practical reach.

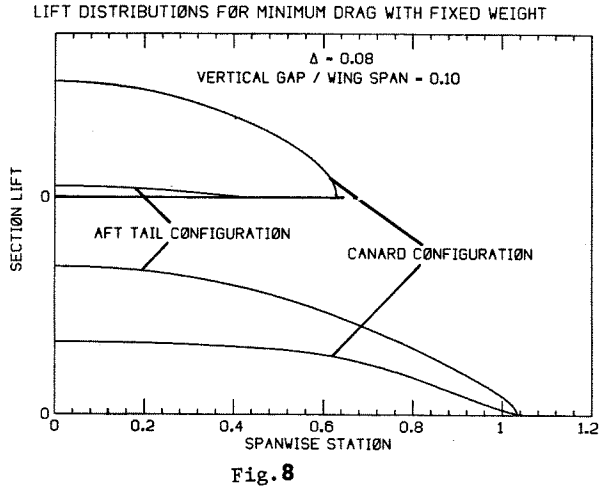

Fig.8

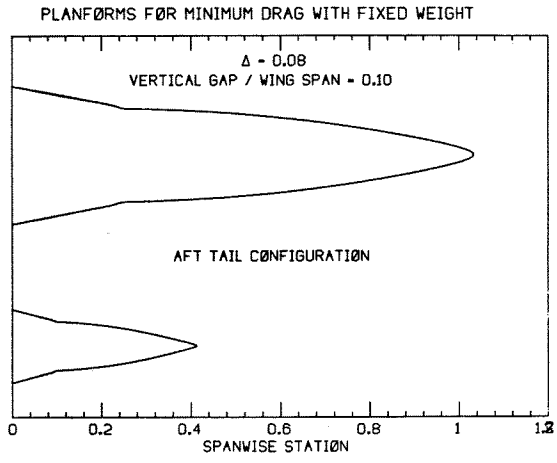

Fig.9

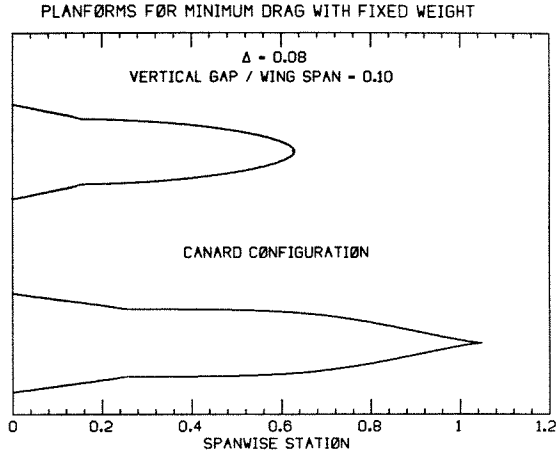

Fig.10

V. Minimum Drag with Stalling Speed Constraint

Previous sections have dealt primarily with the induced drag of lifting systems and have mentioned parasite drag only in passing. Although parasite drag variations with section lift coefficient influence the configuration optimization to some extent, total wetted area directly affects aircraft drag. Fixing the total area, just as fixing the span, is therefore not a rational constraint in an integrated design optimization. Recognizing that not all aircraft are constrained by stalling speed requirements (closely related to landing field length constraints), we nevertheless compare aircraft with constant values of $C_{L_{max}}S$ since, in practice, the minimum lifting surface area is often determined by such a requirement.

Trimmed Maximum Lift Coefficient

Equation (5) reveals that the lift coefficient of the forward surface exceeds that of the aft surface except in cases with very low aspect ratio forward surfaces or very small stability margins. Thus, for configurations with the high aspect ratio canards suggested by the results of the previous section, a large difference between wing and canard C_L exists. (In some of the successful general aviation canard designs the canard is required to achieve nearly twice the C_L of the wing.)

Since it is necessary that the forward surface stall at C_{Lmax} in order that the aircraft exhibit stable behavior at stall, the maximum trimmed lift coefficient (based on total area) is:

$$C_{LAmax} = C_{Lf_{max}} \frac{S_f}{S_{tot}} + C_{Lr} \frac{S_r}{S_{tot}} \tag{9}$$

Figure 10 illustrates the variation of C_{LAmax} with tail span and area ratio. In this figure, the abscissa is the ratio of airplane C_{Lmax} to the maximum lift coefficient of a section with flap, $C_{l_{flap}}$. We have assumed that all of the smaller span and 60% of the larger span's area contains flaps which are capable of increasing the maximum section C_l over that of an unflapped section, C_{l_u}, so that $C_{l_u} = .6C_{l_{flap}}$. This restriction on flapped area is made to accommodate ailerons and 60% is a typical value for conventional aircraft. C_{LAmax} was computed using equations (5) and (9) with the restriction that the aft surface lift coefficient, C_{Lr}, not exceed $C_{Lr_{max}}$ and with:

$$C_{Lw_{max}} = C_{l_{flap}} \frac{S_{flap}}{S_{tot}} + C_{l_u}\left(1 - \frac{S_{flap}}{S_{tot}}\right)$$

With the chosen values of $\frac{S_{flap}}{S_w}$ and $\frac{C_{l_u}}{C_{l_{flap}}}$, $\frac{C_{Lw}}{C_{l_{flap}}} = .84$.

A number of interesting results appear in figure 11. The peaks in the curves of C_{Lmax} vs. $\bar{b}$ occur at small canard aspect ratios for which the wing and canard achieve C_{Lmax} simultaneously. For more reasonable canard aspect ratios, the airplane C_{Lmax} is constrained by the maximum C_L of the canard and in many cases high lift devices on the wing do not increase the aircraft C_{Lmax}. (The part of each curve to the right of the tick mark in figure11 indicates the region in which wing flaps are superfluous.)

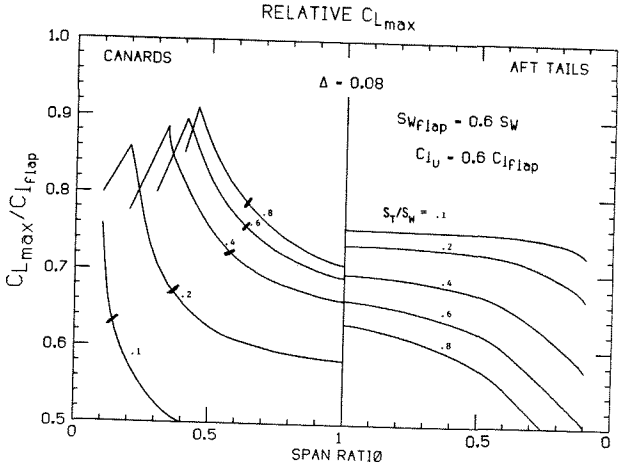

Fig.11

The results for canards summarized in figure 11 are in nearly direct opposition to the induced drag with fixed span results of figures 4 and 5. For high span efficiency, small canards with large span ratios are preferred while large canards with relatively low span ratios lead to high C_{Lmax} The situation for aft tails is more compatible, with small tails leading to high u and high C_{Lmax}. This again illustrates the inadequacies associated with optimal solutions to the various design sub-problems, especially in the case of canard designs.

Total Drag with Fixed Weight and Stalling Speed

The large variations in aircraft C_{Lmax} over the design space covered by these figures leads to differences in total area among aircraft with a specified stalling speed. Changes in total area strongly affect both parasite drag and the span which may achived with a given structural weight. While the relation between total area and aircraft performance depends on the particular aircraft mission the major effects of the stalling speed constraint are illustrated in a comparison of maximum lift-to-drag ratios.

As developed in Appendix II, the ratio of optimum spans of two wings with given structural weight but different areas is:

$$b = S^{1/3}\left(1 + \frac{f_s}{f_b}(1 - S)\right)^{1/3}$$

and if the total drag may be written:

$$D = qSC_{D0} + \frac{W^2}{q\pi b^2 e}$$

then the maximum L/D scales according to:

$$L/D_{max} = S^{-1/6}\left(1 + \frac{f_s}{f_b}(1 - S)\right)^{1/3}$$

Similarly then, the ratio of the trimmed system L/D_{max} to an elliptically-loaded monoplane with $C_{Lmax} = C_{l_{flap}}$ is:

$$L/D_{max} = \frac{C_{Lmax}}{C_{l_{flap}}}^{1/6}\left(1 + \frac{W_s}{W_b}(1 - S)\right)^{1/3}\sqrt{b^2 u}$$

A plot of this parameter (figure 12) reveals a rather broad envelope of near-optimal canard designs. The definite

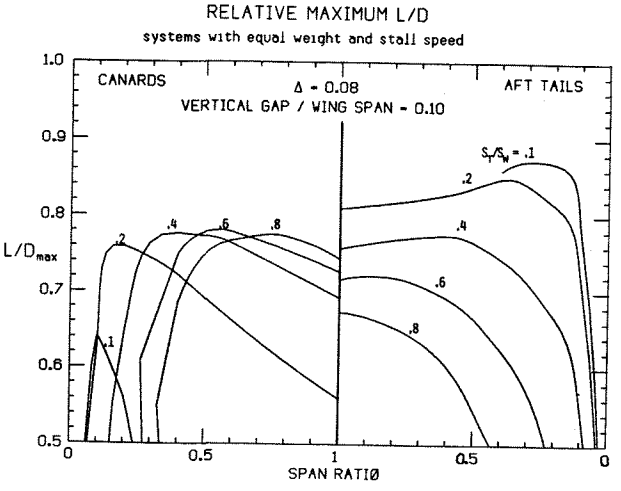

Fig.12

ordering in terms of area ratio is absent in this plot with area ratios of .4 to .8 producing similar L/D_{max} values if the span ratio is properly chosen. Aft-tail designs, on the other hand, preserve the form of the previous figures, reflecting the less competitive demands associated with induced drag, structural weight, and stalling speed.

VI. Off-Design Performance

The lift and chord distributions which minimize induced drag generally require some twisting of the wing. If the distribution of twist is chosen to minimize drag at some design C_L, the lift distribution, and thus the span efficiency, will change with C_L. Similarly, changes in center of gravity position produce changes in $\bar{L}$ and u.

In general, the section lift near the tip of an untwisted wing is larger than desired for minimum drag with fixed weight. The amount of washout required to obtain the lift distributions derived in the previous sections is proportional to C_L and is a function of aspect ratio, sweep, streamwise gap, and the other parameters affecting the optimal lift distribution. With a streamwise gap of 4 wing chords, a C_L of 1.0, and wing aspect ratios of 8 and 12 for the aft-tail and canard designs respectively, the wing of the conventional configuration of figure 10 would require about 6° of washout, while that of the canard design requires nearly 11° to obtain the desired distribution. The smaller spans require only about 3° of twist.

When these twist distributions and tail lift fractions are specified the variation in span efficiency with C_L and $\frac{L_t}{L_{tot}}$ may be written:

$$\frac{1}{u} = \frac{1}{u_0} + k_1\frac{\Delta C_L}{C_L} + k_2\frac{\Delta C_L{}^2}{C_L} + k_3\frac{\Delta L_t}{L_{tot}} + k_4\frac{\Delta L_t{}^2}{L_{tot}} + k_5\frac{\Delta L_t}{L_{tot}}\frac{\Delta C_L}{C_L}$$

where ΔC_L and $\Delta\frac{L_t}{L_{tot}}$ are the deviations from the nominal values and u_0 is the span efficiency with the design lift distributions. Conveniently, $\Delta\frac{L_t}{L_{tot}}$ and the stability margin, Δ, are equivalent variables; changing Δ changes $\Delta\frac{L_t}{L_{tot}}$ by the same amount. Figures 13 and 14 illustrate this function for the two systems, in the form of contours of $\Delta u/u_0$. Note that 1.0 on the $\Delta C_L/C_L$ scale, corresponds to $C_L = \infty$, while $-\infty$ corresponds to $C_L = 0$. The span efficiency is greater than the nominal at higher C_L's since the effectiveness of the twist is reduced in this region, and the lift on each surface is shifted outboard. If the critical loading condition with respect to structural strength occurred at a higher C_L than the nominal value the bending moments would be larger than those used in the weight calculation. Thus, the nominal C_L must be at least as high as that for critical loading. Since this generally occurs at or near $C_L$max, most flying will be in the negative range of $\Delta C_L/C_L$.

In this range, the canard system is somewhat more sensitive to off-design operation than the aft-tailed configuration. Moreover, while the sensitivity of aft-tailed systems varies only slightly with vertical gap, that of canard systems changes quite markedly. If the gap is halved, for example, the sensitivity to $\Delta C_L/C_L$ increases by about 50% although the reduced sensitivity to $\frac{\Delta L_t}{L_{tot}}$ provides some compensation. On the other hand, reducing the canard's span and area reduces the sensitivity to C_L deviations, but increases the sensitivity to tail lift variations. Both types of system are affected quite strongly by sweep, which tends to increase the tip loading and the required washout.

By accepting higher drag at the design C_L, one can make both aft-tailed and canard systems less sensitive to C_L variations. The span efficiency of systems designed for maximum u, rather than maximum b^2u, varies only slightly with C_L. In fact, a system designed for maximum u produces the same drag as a system with the same weight,

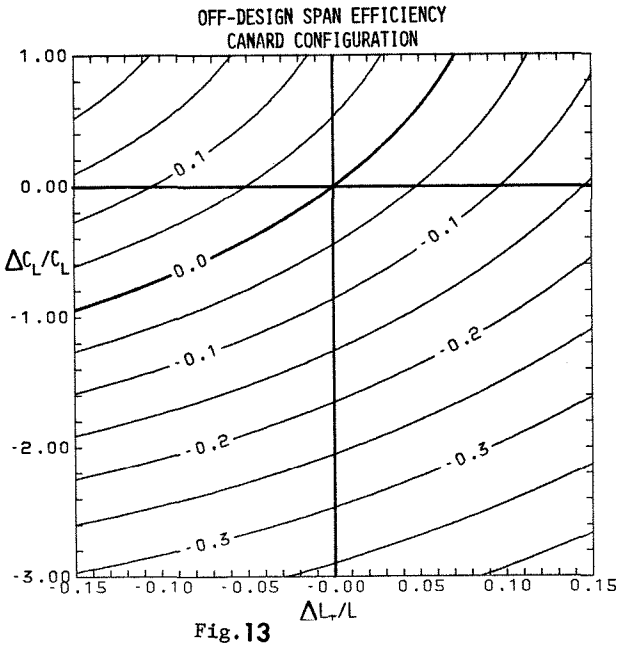

Fig.13

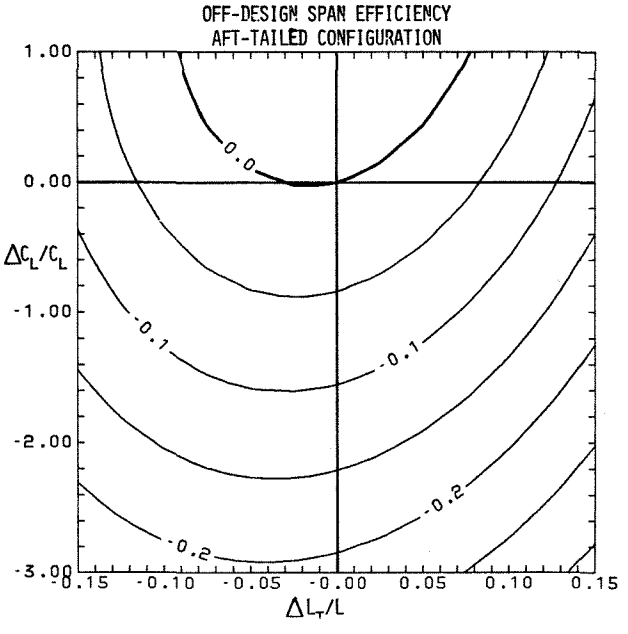

Fig.14

designed for maximum b^2u when $\frac{\Delta C_L}{C_L}$ is roughly -2 to -3 for both aft-tail or canard configurations. In practice these correspond to rather low C_L's— certainly less than 0.5 and perhaps as little as 0.25. Of course induced drag at these C_L's is such a small fraction of the total that the difference between the two systems would hardly matter. At higher C_L's, however, the performance of the system with maximum b^2u would be substantially better and thus superior, overall, despite its relatively high sensitivity to off-design operation.

VII. Conclusions

The analyses presented here are intended to provide an indication of some of the fundamental considerations involved in the preliminary design optimization of canard configurations. In practice, many factors which were neglected in this paper strongly influence the design. Fuselage weight differences, flap system cost and complexity, landing gear placement, propulsion system integration, handling qualities criterion, and additional controllability requirements are among the perhaps less fundamental, but often vitally important aspects of preliminary design which are more difficult to quantify. The goal of fundamental analyses such as these, however, is to isolate the most important factors so that their effects may be seen clearly and many of the issues discussed here are central to the design of subsonic canard configurations and to comparisons with conventional designs.

1) The induced drag analysis of section II provides a practical means of estimating the minimum induced drag of canard designs. It reduces simply to Prandtl's biplane equation, providing a reasonable bounds for the induced drag which may be achieved in practice.

2) The stability and trim constraints place severe demands on canard configurations, generally forcing the canard surface to carry a disproportionate share of the total lift, and resulting in low span efficiencies unless the canard span is large. (Canard designs would benefit from relaxed static stability requirements to a greater extent than would conventional designs.)

3) The maximum lift coefficient obtainable with canard configurations is, in some cases, larger than those which may be obtained with conventional designs but these cases suffer very large induced drag penalties so that in most practical cases, little difference in C_{Lmax} exists.

4) Although the total induced drag for fixed span may be reduced in some cases by reducing the vertical gap, structural weight and off-design considerations suggest that the vertical gap should be large.

5) Canard configurations exhibit higher sensitivity to changes in center of gravity position and C_L than aft-tail designs, illustrating some of the limitations of the minimum induced drag relation and the utility of twist–changing flaps.

6) The optimization of canard configurations is made difficult by several factors (e.g. C_{Lmax} vs. induced drag, induced drag vs. structural weight), which act in concert for conventional designs but in direct competition for the canard case. Thus, compromises are necessary in canard designs and variations in mission requirements are likely to produce greater variations in "optimal" geometry for these unconventional aircraft.

VIII. References

1) Lamar,J.E., "A Vortex Lattice Method for the Mean Camber Shapes of Trimmed Non–Coplanar Planforms with Minimum Vortex Drag," NASA TN-D 8090, 1976.

2) Blackwell, J.,"Numerical Method To Calculate the Induced Drag or Optimal Loading for Arbitrary Non–Planar Aircraft," NASA SP-405, May 1976.

3) McLaughlin, M., "Calculations, and Comparison with an Ideal Minimum of Trimmed Drag for Conventional and Canard Configurations Having Various Levels of Static Stability," NASA TN-D-8391, 1977.

4) Von Karman, T., and Burgers, J.M.: General Aerodynamic Theory – Perfect Fluids, Vol.II of Aerodynamic Theory, W.F. Durand, ed., Dover Edition, N.Y., 1963.

5) Prandtl, L., "Induced Drag of Multiplanes," NACA TN-182, March 1924.

6) Laitone, E., "Positive Tail Loads for Minimum Induced Drag of Subsonic Aircraft," Journal of Aircraft, Vol. 15, Dec. 1978, pp. 837-842.

7) Laitone, E., "Prandtl's Biplane Theory Applied To Canard and Tandem Aircraft," Journal of Aircraft, Vol.17, April 1980, pp.233-237.

8) Sachs, G., "Minimum Trimmed Drag and Optimum C.G. Position," Journal of Aircraft, Vol.15, Aug. 1978, pp. 456-459.

9) Butler, G.F. "Effect of Downwash on the Induced Drag of Canard – Wing Combinations," Journal of Aircraft, Vol. 19, May 1982, pp.410-411.

10) Munk, M., "Minimum Induced Drag of Airfoils," NACA Rpt. 121, 1921.

11) Feistal, T., Corsiglia, V., and Levin, D., "Wind-Tunnel Measurements of Wing-Canard Interference and a Comparison with Various Theories," SAE Tech. Paper 810575, April 1981.

12) Reid, E.G., Applied Wing Theory, McGraw-Hill, New York, 1932.

13) Jones, R.T., Cohens, D., High Speed Wing Theory, Princeton University Press, Princeton, N.J., 1960, pp.62-63.

14) Prandtl, L.,"Uber Tragflugel des Kleinsten Induzierten Widerstandes," Zetshrift fur Flugtechnik und Motorluftschffahrt 24 Jg. 1933. (Reprinted in Tollmein, W., Schlichting, H., and Gortler, H., ed., Gesammelte Abhandlungen, Springer–Verlag, 1961.)

15) Jones,R.T., "The Spanwise Distribution of Lift for Minimum Induced Drag of Wings Having a Given Lift and Root Bending Moment," NACA TN-2249, 1950.

16) Jones, R.T., "Effect of Winglets on the Induced Drag of Ideal Wing Shapes," NASA TM 81230, 1980.

IX. Nomenclature

AR	aspect ratio, $\frac{b^2}{S}$
b	span
$\bar{b}$	span ratio, $\frac{b_t}{b_w}$
c	chord
C_{D0}	zero lift drag coefficient
C_l	section lift coefficient
$C_{L\alpha}$	lift curve slope
C_m	pitching moment coefficient
D	drag
e	Oswald efficiency factor
f	weight fraction
h	vertical gap
$\bar{h}$	non-dimensional gap, $\frac{h}{b_w}$
L	lift
$\bar{L}$	lift ratio, $\frac{L_t}{L_w}$
l	section lift
M	bending moment
q	dynamic pressure
u	span efficiency
W	weight
w	weight per unit span
Δ	stability margin
μ	structural weight constant
σ	interference factor
χ	nondimensional chord

Subscripts

ac	aerodynamic center
b	spar cap component
f	forward surface
$flap$	value for flapped section
r	rear surface
s	surface skin component
t	tail (or smaller span)
u	value for unflapped section
w	wing (or larger span)

Appendix I
Minimum Induced Drag of Wing / Tail Systems

The induced drag of two interfering surfaces in incompressible flow may be written:

$$D_i = \int_{wing} \epsilon_w l_w(y)dy + \int_{tail} \epsilon_t l_t(y)dy + \int_{tail} \epsilon_{wt} l_t(y)dy \quad (1A)$$

with ϵ_w the downwash angle produced at the wing (larger span) by the wing's trailing vortex system and ϵ_t, the downwash angle at the tail due to the tail's loading. ϵ_{wt} is the downwash angle produced by the wing's trailing vorticity over the tail's projection infinitely far downstream (Trefftz plane). Munk's stagger theorem permits the interference drag to be written as a single term and also assures that equation (1A) is applicable to canard or aft-tail configurations.

When the wing and tail lift distributions are expanded as in equation 2 where θ_w and θ_t are the spanwise angle variables:

$$y = \frac{b_w}{2}cos\theta_w = \frac{b_t}{2}cos\theta_t$$

the integrations of equation (1A) yield:

$$D_i = \frac{L^2}{q\pi {b_w}^2}\sum m{A_{mw}}^2 + \frac{1}{\bar{b}^2}\sum n{A_{nt}}^2$$

$$+\frac{2}{\bar{b}}\sum\sum A_{nt}A_{mw}T_{mn}(\bar{b},\bar{h}) \quad (1B)$$

where T_{mn} is the Trefftz plane downwash integral associated with the third term of equation (1A) over the n^{th} harmonic of the wing lift and m^{th} harmonic of the tail's lift distribution. (Space does not permit a detailed discussion of the evaluation of T_{mn} but some discussion may be found in the listed references.)

Since the coefficients A_{w1} and A_{t1} are specified by:

$$\frac{L_w}{L} = A_{w1}$$

$$\frac{L_t}{L} = A_{t1}$$

we define a vector of unknown harmonic coefficients:

$$A = [A_{w3}, A_{w5}, ...A_{wM}, A_{t3}, A_{t5}, ...A_{tN}]^T$$

so that equation (1B) becomes:

$$q\pi D_i = \frac{{L_w}^2}{{b_w}^2} + \frac{{L_t}^2}{{b_t}^2} + \frac{2L_wL_tT_{11}}{b_tb_w} + A^T\left(T'A + \frac{2L_w}{L}T'_w + \frac{2L_t}{L}T'_t\right) \quad (1C)$$

where:

$$T' \equiv \begin{bmatrix} 3 & 5 & \cdots & & T_{ji}/\bar{b} \\ & & & M & \\ T_{ij}/\bar{b} & & & 3/\bar{b}^2\ 5/\bar{b}^2 & \cdots\ N/\bar{b}^2 \end{bmatrix} \quad \begin{matrix} i = 3, 5, \ldots N \\ j = 3, 5, \ldots M \end{matrix}$$

and:

$$\bar{b}T_w' = [0, 0, ...0, T_{13}, T_{15}, ...T_{1N}]^T$$

$$\bar{b}T_t' = [T_{31}, T_{51}, ...T_{M1}, 0, 0, ...0]^T$$

The first three terms of equation (1C) include the effects of the first harmonics and are therefore just the terms in equation 1 of section II. The minimum induced drag is

obtained by setting the gradient of the additional term to 0:

$$\nabla D_i = 2(T'A + \frac{L_w}{L}T_w' + \frac{L_t}{L}T_w') = 0$$

or:

$$A = -[T']^{-1}(\frac{L_w}{L}T_w' + \frac{L_t}{L}T_w')$$

Defining:

$$T_w'' = -[T']^{-1}T_w'$$

$$T_t'' = -[T']^{-1}T_t'$$

we obtain:

$$A = \frac{L_w}{L}T_w'' + \frac{L_t}{L}T_t''$$

And substitution into (1C) produces:

$$q\pi D_i = \frac{L_w{}^2}{b_w{}^2}\sigma_w + \frac{L_t{}^2}{b_t{}^2}\sigma_t + \frac{2L_wL_t}{b_tb_w}\sigma_{wt} \qquad (1D)$$

with:

$$\sigma_w = 1 + T_w'T_w''$$

$$\sigma_t = 1 + T_t'T_t''$$

$$\sigma_{wt} = T_{11} + \frac{1}{2}T_w'T_w'' + \frac{1}{2}T_t'T_t''$$

In practice 5 to 9 harmonics are sufficient to represent the required lift distributions for most cases. In extreme cases with low span and gap ratios M = 21 and N = 5 produce reasonable accurate solutions.

Appendix II.
Minimum Induced Drag with Fixed Weight

The expression for the weight of a two-surface system relative to that of a reference monoplane given in section IV is:

$$W = f_sS + \frac{f_bb_w{}^3}{S}(\sum_1^M A_{wm}B_{wm} + \bar{b}^3\sum_1^N A_{tn}B_{tn}) \qquad (2A)$$

When this weight is held constant (along with total area, planform shape—through B, tail lift fraction, and total lift) the variables to be determined include the span and the amplitudes of the lift distributions' higher harmonics.

If the span is specified and free variables written in vector form as in the preceeding section, the weight constraint becomes:

$$\frac{\mu}{b_w{}^3} = \frac{W - f_sS}{f_b}\frac{S}{b_w{}^3} = A_{w1}B_{w1} + \bar{b}^3A_{t1}B_{t1} + A^TB \qquad (2B)$$

where:

$$B = [B_{w3}, B_{w5}, ..., B_{wM}, \bar{b}^3B_{t3}, \bar{b}^3B_{t5}, ..., \bar{b}^3B_{tN}]^T$$

When the weight constaint is appended to the expression for induced drag with a Lagrange multiplier and we include only terms dependent on A, the quantity to be minimized is:

$$D' = \frac{1}{b_w{}^2}A^TT'A + \frac{2L_w}{L}T_w' + \frac{2L_t}{L}T_t' \qquad (2C)$$

setting $\nabla D' = 0$:

$$0 = T'A + \frac{L_w}{L}T_w' + \frac{L_t}{L}T_t' + \frac{b_w{}^2\nu}{2}B \qquad (2D)$$

If we introduce:

$$\Delta A = -[T']^{-1}B$$

then:

$$A = \frac{L_w}{L}T_w'' + \frac{L_t}{L}T_t'' + \frac{b_w{}^2\nu}{2}\Delta A \qquad (2E)$$

Where T_w'' and T_t'' are defined in appendix I.

Substitution into equation 2B eliminates ν from 2E. Now if $b_w{}^*$ denotes the span at which the solution for minimum induced drag with fixed span satisfies the weight constraint then:

$$A = \frac{L_w}{L}T_w'' + \frac{L_t}{L}T_t'' + \frac{(\frac{\mu}{b_w{}^3} - \frac{\mu}{b_w{}^{*3}})\Delta A}{B^T\Delta A} \qquad (2F)$$

substituting this expression into the expression (1C) for induced drag provides an explicit relationship between drag and span with fixed weight:

$$q\pi D_i = \frac{L_w{}^2}{b_w{}^2}\sigma_w + \frac{L_t{}^2}{b_t{}^2}\sigma_t + \frac{2L_wL_t}{b_tb_w}\sigma_{wt} - \frac{L^2}{b_w{}^2}\frac{(\frac{\mu}{b_w{}^3} - \frac{\mu}{b_w{}^3})^2}{B^TA} \qquad (2G)$$

Although this function, in many cases, has a minimum with respect to b_w with b_w somewhat larger than $b_w{}^*$, in some cases the function decreases monotonically with b_w. Inspection of equation 2G also shows that D_i approaches zero as span becomes infinitely large. Part of this unusual behavior reflects a limitation of the weight model which is valid only for lift distributions for which the local bending moment does not change sign over the span of the surface. However, cases which exhibit monotonic behavior with b_w would indeed offer lower drag for a fixed weight with negatively loaded tips (provided that one could maintain this load distribution in the critical flight condition). In such cases, the optimum span is taken, for the purposes of this analysis, as that span at which the tip loading becomes negative.

Both the true minimum with respect to span and the transition from positive to negative tip loading occur at characteristic values of $\frac{\mu}{b_w{}^3}$. Thus for any value of μ the optimum span is given by the relation:

$$\frac{\mu}{b_w{}^3} = \frac{\mu}{b_w{}^3}_{opt} = f(L, \bar{L}, \bar{b}, \bar{h})$$

So if f_s, S, or W are varied, the optimum span scales as:

$$b_w{}^3 = \frac{\frac{W - f_sS}{f_b}S}{(\frac{\mu}{b_w{}^3})_{opt}}$$